

# Discrete Abstractions for Manufacturing Logistics Optimization for the Food Service Industry\*

Anatoli A. Tziola and Savvas G. Loizou

**Abstract**—This paper presents an analysis under a formal methods framework for multi-agent systems applications in manufacturing logistics optimization. More specifically, a case study for workflow abstraction for manufacturing logistics optimization is presented utilizing the SPECTER task planner framework for a food service company. A workflow abstraction is constructed considering the workflow stages, the temporal costs (i.e. a machine operation, products time construction, worker transitions between work-cells) and the agents involved in the production line (such as robots, machines, humans, materials, products etc.). Based on the derived abstraction, different case studies are investigated and sub-optimal solutions are provided. The paper leverages the modeling power of the SPECTER framework, while demonstrating its potential applications in providing solutions for the food service industry.

## I. INTRODUCTION

Automation and optimization of manufacturing logistics tasks has been one of the major areas of research interest during the last decades. In particular, discrete optimization problems have a wide variety of applications in the field. Applications of formal methods to discrete optimization problems provide for discrete abstractions, modeling the continuous agents' actions in an appropriate discrete domain. Task planning is usually considered in the discrete domain where given an initial state and goal, the task planner aims to generate a sequence of intermediate tasks to guide a team of agents (robots, workers, machines, etc.) to accomplish the goal. Several research works address the challenges of task and motion task planning problems utilizing discrete abstractions and temporal logic [1]–[7].

Some of the state-of-art optimization tools are: the Gurobi optimizer [8], a Mixed Integer Programming (MIP) solver supporting quadratic objectives; the NVIDIA cuOpt [9] that employs GPU-accelerated logistics solvers relying on heuristics, metaheuristics and optimization with constraints; the Quantum-inspired annealers such as Fujitsu Digital Annealer (DA3) [10] for quadratic unconstrained binary optimization (QUBO) problems; and Fixstars Annealer Engine (AE) [11], a Cloud Platform for Quantum Annealing using GPUs; the OpenJij [12], a heuristic optimization library that offers solutions to Quadratic Unconstrained Optimization Problem (QUBO) and Ising models.

\*This work was partially supported by European Union's research and innovation programs under grant agreements 951813 (Better Factory/H2020) and 101092295 (CIRCULOOS/Horizon Europe).

The authors are with the Department of Mechanical Engineering and Materials Science and Engineering, Cyprus University of Technology, Limassol, CYPRUS, {anatoli.tziola, savvas.loizou}@cut.ac.cy.

This paper presents an application of the task planning framework proposed by the authors at [13]. Potential applications of SPECTER framework could be found also in [14]. This work focuses on the presentation of the discrete abstraction models of a manufacturing workflow and how different abstractions of the same workflow could reduce the model's state space. Due to data confidentiality obligations, we have to keep the process data anonymized. Although we understand that anonymization poses a challenge to the presentation of this work, special effort was taken to present it in a meaningful way, while ensuring that no sensitive information is revealed.

The objective of the Food Service Industry under consideration was to optimize the workflow process and overcome the manufacturing challenges by reducing waste and the time required for reconfiguration of the production. In this paper, different scenarios were investigated depending on the available resources, robotic agents and temporal costs of the workflow processes in order to determine the optimal number of the agents required for the final product manufacturing and the sequence of actions that need to be performed by those agents. Through the SPECTER task planner implementation, the industry could identify a better agent allocation in the production line, while the optimum number of agents required to perform the necessary tasks is specified.

The rest of the paper is organized as follows: Section III presents the modeling of the workflow while section IV presents the environment and agents modeling using the  $\epsilon_0$ -NFA formalism. Section V presents the case studies and Section VI concludes the paper.

## II. DEFINITIONS OF TERMS

To ensure a common understanding of the terminology used throughout this work, a definition of terms that are frequently used in this work is provided.

Agents are considered as the autonomous entities in the manufacturing workflow that are acting/reacting to their surroundings during a process or trigger event while being influenced by other agents. Agents could be robots, AGVs, humans, machines, materials, products, work-cells, work stations etc. In this work, we are not focusing on the processes carried out in each work-cell, but rather on considering the abstract of the process workflow of each work-cell taking into account all agents involved in it. Therefore, each agent has individual capabilities and constraints while there are inter-agent capabilities and constraints that emerge when multiple agents are present. The environment model captures

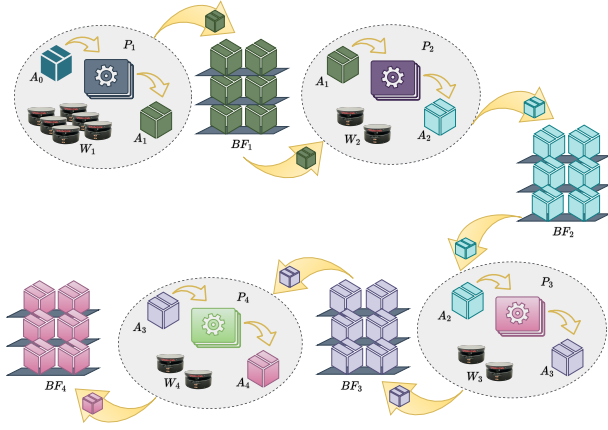


Fig. 1: Diagram of the manufacturing workflow.

the full behavior of the system derived from the capabilities and constraints of the agents involved in it.

The discrete models of the environment and the agents involved in it are constructed utilizing the formal framework of  $\epsilon_0$ -NFAs [13], in order to model the behavior of the system at any time instant. To this goal, we construct the environment automaton based on the agents' capabilities and constraints taking into account the inter-agent capabilities and constraints that emerge when multiple agents are present. The detailed description on the environment and the agents models construction could be found in [13]. The environment and agents models are constructed only once and then, any task specification from any initial condition can be solved.

### III. MANUFACTURING WORKFLOW MODELING

In this work, a cellular layout arrangement entailing 4 different work-cells is considered. Each work-cell contains a certain number of machines, equipment and supplies. Each process of a work-cell requires a specific number of robotic agents for the processes to be performed. The robotics agents involved in a work-cell are grouped in a team. Temporal costs associated to each work-cell refer to the production of 1 unit product per hour. Buffer zones are considered as the logistics facilities set up near the production work-cells that serve to temporarily store semi-finished or finished products. We considered 4 buffer zones, 1 for each work-cell. Products manufactured in a work-cell are stored at the buffer zone related to the work-cell. The maximum capacity of each buffer is 2 units. The diagram of the manufacturing workflow is presented in Fig.1.

Let  $P_1$ ,  $P_2$ ,  $P_3$  and  $P_4$  represent the work-cells of the manufacturing workflow and  $BF_1$ ,  $BF_2$ ,  $BF_3$  and  $BF_4$  be the buffer zones related to each work-cell. Assuming that the factory utilizes unprocessed material  $A_0$  to construct the semi-finished products  $A_1$ ,  $A_2$ ,  $A_3$  and manufactures the final product  $A_4$ . Moreover,  $BF_1$  represents the buffer zone for semi-finished products  $A_1$ ,  $BF_2$  the buffer for  $A_2$ ,  $BF_3$  the buffer for  $A_3$  and  $BF_4$  the buffer for  $A_4$ . The company

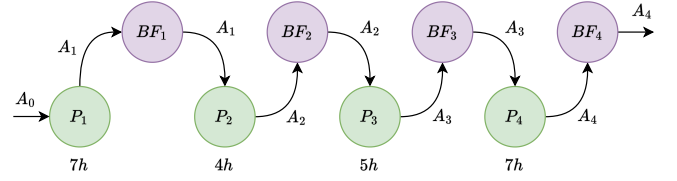


Fig. 2: Workflow abstraction. Numbers below nodes indicate duration (hours).

allots 10 robots for this workflow. The minimum number of robots required for the production of 1 unit of  $A_4$  is 6.

The work-cells of the production workflow with its individual temporal costs, the number of robots involved in each work-cell, and the input and output products of each work-cell are presented in Table I. The workflow process is considered as follows: In work-cell  $P_1$ , 6 robots are involved in order to produce 1 unit of semi-finished product  $A_1$  after 7 hours using 1 unit of material  $A_0$ . The units of  $A_1$  are stored at  $BF_1$ . In work-cell  $P_2$ , 2 robots are involved in order to produce 1 unit of semi-finished product  $A_2$  after 4 hours using 1 unit of semi-finished product  $A_1$  retrieved from  $BF_1$ . The units of  $A_2$  are stored at  $BF_2$ . In work-cell  $P_3$ , 2 robots are involved in order to produce 1 unit of semi-finished product  $A_3$  after 5 hours using 1 unit of semi-finished product  $A_2$  retrieved from  $BF_2$ . The units of  $A_3$  are stored at  $BF_3$ . In work-cell  $P_4$ , 2 robots are involved in order to produce 1 unit of final product  $A_4$  after 7 hours using 1 unit of semi-finished product  $A_3$  retrieved from  $BF_3$ . The units of  $A_4$  are stored at  $BF_4$ .

Work-cell	$P_1$	$P_2$	$P_3$	$P_4$
Temporal cost	7	4	5	7
Number of robots	6	2	2	2
Input products	$A_0$	$A_1$	$A_2$	$A_3$
Output products	$A_1$	$A_2$	$A_3$	$A_4$

TABLE I: Work-cells with costs and robots involved.

### IV. ABSTRACTION MODEL OF MANUFACTURING WORKFLOW

The abstraction model of the workflow is required to cast the problem in the discrete processes domain of the SPECTER framework. The agents considered for the workflow abstraction are: the robotics agents grouped in teams (1 team is considered as 1 agent), buffer zones, materials, semi-finished and final products. The workflow abstraction is illustrated in Fig. 2. The nodes of the diagram represents the work-cells and buffer zones, whereas the arrows indicate the input and the output products of each work-cell and buffer zone.

#### A. Agent modeling: Robots

The robotic agents could be grouped in teams of 6 or 2 agents. For the work-cell  $P_1$ , 6 robotic agents are required. Thus, a team of 6 robotic agents or 3 teams of 2 robotic agents are required for the work-cell  $P_1$ . Those two approaches determine two different abstractions, that will be

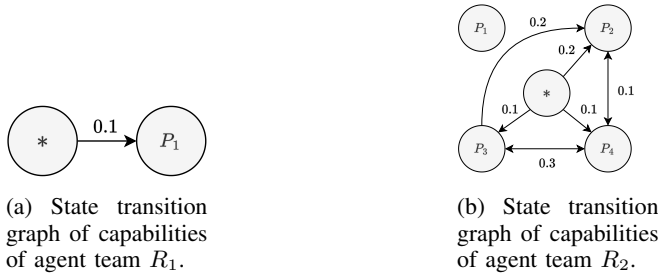


Fig. 3: State transition graph of capabilities of robots teams.

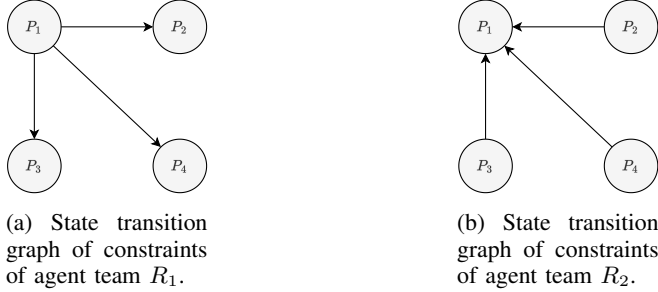


Fig. 4: State transition graph of constraints of robots teams.

exploited in the sequel. For the work-cells  $P_2$ ,  $P_3$  and  $P_4$ , 1 team of 2 robotic agents is required.

Let  $R_1$  denote the team of 6 robots and  $R_2$  denote the team of 2 robots. The state set of the team  $R_1$  is  $X_{R_1} = \{*, P_1\}$ ,  $X_{R_2} = \{*, P_1, P_2, P_3, P_4\}$  for  $R_2$ . The work-cells are considered as robots' states while the  $*$  indicates that robots could be anywhere in the factory. Thus, the state transition graphs of the capabilities of the robots teams are as depicted in Fig 3. The numbers on the edges represent the temporal costs for the transitions. The constraints of the robot teams are illustrated in Fig. 4.

The capabilities of robots team  $R_1$ , shown in Fig. 3a, presents that the team  $R_1$  could navigate at work-cell  $P_1$  from anywhere in the factory. The capabilities of  $R_2$ , shown in Fig. 3b, presents that the team  $R_2$  could navigate at work-cell  $P_2$ ,  $P_3$ ,  $P_4$  from anywhere in the factory.

The constraints of robots team  $R_1$ , shown in Fig. 4a, presents that the team  $R_1$  is not allowed to navigate and perform actions at  $P_2$ ,  $P_3$  and  $P_4$ , since the processes of work-cells  $P_2$ ,  $P_3$  and  $P_4$  require exactly 2 robots to be performed. The constraints of robots team  $R_2$ , shown in Fig. 4b, presents that the team  $R_2$  is not allowed to navigate and perform actions at  $P_1$ , since the processes of work-cell  $P_1$  require exactly 6 robots in order to be performed.

To construct the models of robots team  $R_1$ , the constraints  $\epsilon_0$ -NFA of  $R_1$  is subtracted from the capabilities  $\epsilon_0$ -NFA of  $R_1$ . To construct the models of robots team  $R_2$ , the constraints  $\epsilon_0$ -NFA of  $R_2$  is subtracted from the capabilities  $\epsilon_0$ -NFA of  $R_2$ .

### B. Agent modeling: Materials, semi- and finished products

The state transition graphs of the material  $A_0$ , the semi-finished products  $A_1$ ,  $A_2$ ,  $A_3$  and the final product  $A_4$  are depicted in Fig. 5. The work-cells and buffer zones are

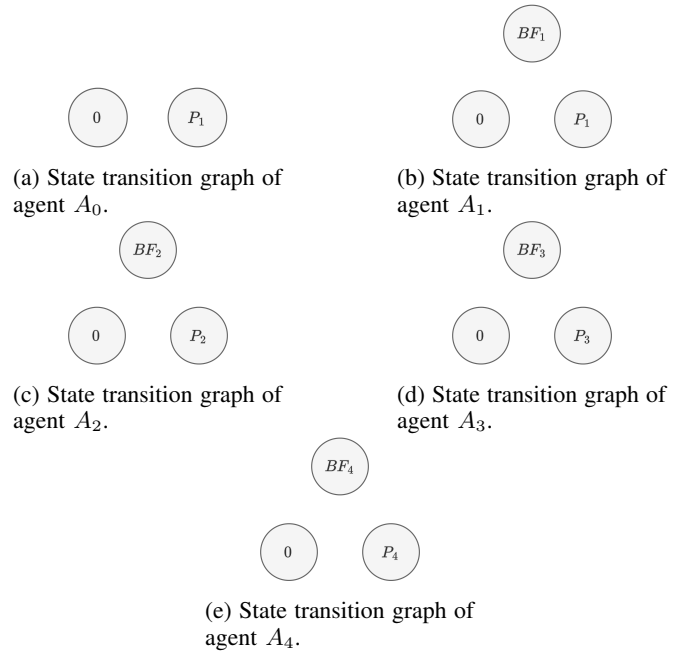


Fig. 5: State transition graphs of unprocessed material  $A_0$  (5a), semi-finished product  $A_1$  (5b), semi-finished product  $A_2$  (5c), semi-finished product  $A_3$  (5d), final product  $A_4$  (5e).

considered as states. The transitions of  $A_0$ ,  $A_1$ ,  $A_2$ ,  $A_3$  and  $A_4$  are enabled through the inter-agent capabilities. The state set of  $A_0$  is  $X_{A_0} = \{0, P_1\}$ ,  $X_{A_1} = \{0, P_1, BF_1\}$  of  $A_1$ ,  $X_{A_2} = \{0, P_2, BF_2\}$  of  $A_2$ ,  $X_{A_3} = \{0, P_3, BF_3\}$  of  $A_3$  and  $X_{A_4} = \{0, P_4, BF_4\}$  of  $A_4$ . In the automata, the state "0" indicates that there is no available resources of the specific product.

An agent model is constructed by subtracting the agent's constraints from the agent's capabilities. We repeat the procedure for each agent to get the models of all agents.

Utilizing the concatenation operation on the agent's capabilities and constraints expressed as  $\epsilon_0$ -NFAs, we construct the model of the environmental capabilities and environmental constraints expressed as  $\epsilon_0$ -NFAs.

Let  $n$  be the total number of agents, then an environmental state consists of  $n$  elements such that a specific projection of an environment's state indicates the state of each agent in any time instant. We can now proceed with the modeling of inter-agent capabilities and inter-agent constraints.

### C. Agent modeling: Buffer zones

Fig. 6 models the state transition graph of a buffer zone in the production line. The transitions in the buffer zone model are enabled through the inter-agent capabilities.

### D. Inter-agent capabilities

Inter-agent capabilities enable the processes procedures to construct the semi-finished and the final products, while defining the inter-agent capabilities between agents  $A_0$ ,  $A_1$ ,  $A_2$ ,  $A_3$ ,  $A_4$ ,  $R_1$ ,  $R_2$ . Assuming that the robots are grouped in 4 teams with the 1st the team  $R_1$  of 6 robots, the team

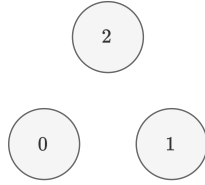


Fig. 6: State transition graph of agent  $BF_1$ .

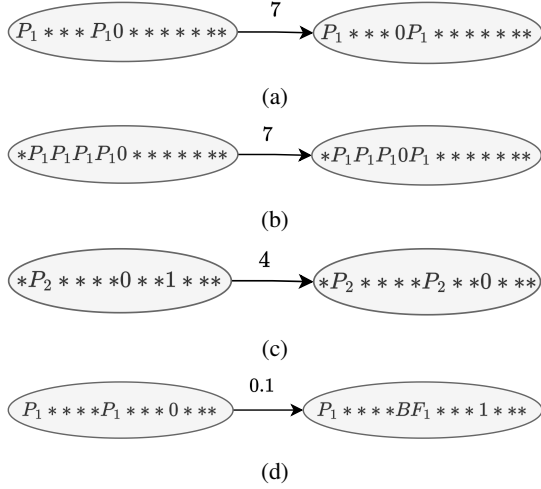


Fig. 7: State transition graphs of inter-agents capabilities.

$R_2$  be the 2nd team of 2 robots, the team  $R_3$  be the 3rd team of 2 robots and  $R_4$  be the 4th team of 2 robots. The capabilities and constraints of robots teams  $R_3$  and  $R_4$  are modeled as in Fig. 3b and Fig. 4b, respectively. A sample of the environmental states transitions are illustrated in Fig. 7. The agent's state indicated by \* means that the agent state is not considered in this inter-agent capability, in the sense of the agent state could take any value of the agent's state space.

Fig. 7a models the production of semi-finished product  $A_1$  utilizing the team  $R_1$  of 6 robots performing actions at work-cell  $P_1$  using material  $A_0$ . The transition shows that the  $A_1$  is produced at  $P_1$  after 7 hours. Fig. 7b models the production of semi-finished product  $A_1$  utilizing the teams  $R_2$ ,  $R_3$  and  $R_4$ , 6 robots in total grouped in 3 teams of 2 robots. This inter-agent capability enables the capability transition of  $R_2$ ,  $R_3$  to  $P_1$  simultaneously. Fig. 7c models the production of semi-finished product  $A_2$  in 4 hours using semi-finished product  $A_1$  retrieved from buffer zone  $BF_1$  utilizing the robots team  $R_2$ . Fig. 7d models the loading of  $A_1$  produced at  $P_1$  at buffer zone  $BF_1$  by team robots  $R_1$  in 10 minutes.

#### E. Inter-agent constraints

Fig. 8a presents a sample of inter-agent constraints. This constraint represents that the presence of all teams at work-cell  $P_1$  at the same time is forbidden. Fig. 8b models the constraint of robots teams  $R_2$ ,  $R_3$  and  $R_4$  to be present at  $P_2$  at the same time.

Utilizing the union operation on the environmental capabilities and inter-agent capabilities, we construct the global

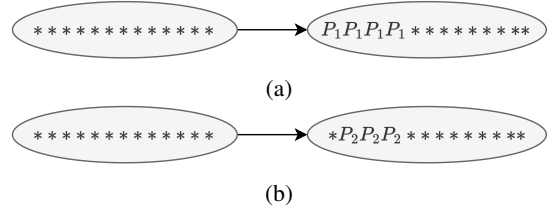


Fig. 8: State transition graphs of inter-agent constraints.

capabilities. Utilizing the union operation on the environmental constraints and inter-agent constraints, we construct the global constraints. Subtracting global constraints from global capabilities through the subtraction operation, we construct the environment model  $\epsilon_0 S$  expressed as  $\epsilon_0$ -NFA.

Having the environment model, we can state the objective (called as task specification [13]) that is defined as a projection of the environment's state space that indicates the desired state of specific agent(s) in the multi-agent system.

## V. CASE STUDIES

Two different case studies presenting the 2 different abstractions (see Section IV-A.) were investigated. In each case study, different scenarios were implemented utilizing 6, 8 and 10 robots in the production line. Case studies were implemented on a computer with AMD Ryzen 5 4500U 2.3 GHz and 16GB RAM. In the case studies A-I, A-II and A-III, the robots are grouped in teams of 2 robots, whereas in the case studies B-I and B-II, the robots are grouped both in a team of 6 and teams of 2 robots. A time limit of one hour was set for the computation of the (sub-)optimal solution utilizing the heuristic algorithm of [13].

We assume that there are unlimited resources of unprocessed material  $A_0$  at  $P_1$ . For the initial conditions, we assume that semi-finished products  $A_1$ ,  $A_2$  and  $A_3$  and final product  $A_4$  have not been produced yet. Buffer zones serve products transportation between work-cells. Robots are allowed to retrieve products from the buffer zones only.

Assuming that the buffer zones, the material and the products models are the same for all case studies, then the models of these agents are considered as follows. The state transition graphs of capabilities and constraints of each robots team are defined as in Fig. 3b and Fig. 4b, respectively. Each buffer zone is modeled as in Fig. 6, while the products  $A_0$ ,  $A_1$ ,  $A_2$ ,  $A_3$ ,  $A_4$  are modeled as in Fig. 5. Using the agents' capabilities (Fig. 3a, 3b), agents' constraints (Fig. 4a, 4b), inter-agent capabilities (Fig. 7) and inter-agent constraints (Fig. 8), we construct the agents' and the environment model for each case study.

#### A. Case study A-I

For the first case study, we considered 12 agents; material  $A_0$ , semi-finished products  $A_1$ ,  $A_2$ ,  $A_3$ , final product  $A_4$ , buffer zones  $BF_1$ ,  $BF_2$ ,  $BF_3$ ,  $BF_4$  and 6 robots in total grouped in 3 teams of 2. The 3 teams together could perform actions in work-cell  $P_1$ , since 6 robots are required. However, each team is allowed to perform actions in work-cells  $P_2$ ,

$P_3$  and  $P_4$ , since 2 robots are required in each work-cell. Let  $R_2$ ,  $R_3$  and  $R_4$  be the robots teams utilized. The objective is to produce 2 units of  $A_4$  and locate it at  $BM4$  utilizing the 6 robots in the production line.

In the solution computed by SPECTER, the objective is fulfilled in 25 steps for the concurrent task execution. In the 1st step  $T_1$ , the teams  $R_2$ ,  $R_3$ ,  $R_4$  goes at work-cell  $P_1$ . In step  $T_2$ , the process in  $P_1$  is started utilizing material  $A_0$ . In  $T_3$ ,  $A_1$  is produced after 7 hours. In  $T_4$ ,  $A_1$  is stored at  $BF_1$  ( $BF_1$  capacity = 1 unit). In  $T_5$ ,  $R_2$  goes at  $P_2$ . In  $T_6$ , the process at  $P_2$  is started utilizing 1 unit from  $BF_1$  ( $BF_1$  capac. = 0). In  $T_7$ ,  $A_2$  is produced at  $P_2$  after 4 hours. In  $T_8$ ,  $A_2$  are stored at  $BF_2$  ( $BF_2$  capac. = 1 unit). In  $T_9$ , the teams  $R_2$ ,  $R_3$ ,  $R_4$  goes at work-cell  $P_1$ . In  $T_{10}$ , the process in  $P_1$  is started utilizing material  $A_0$ . In  $T_{11}$ ,  $A_1$  is produced after 7 hours. In  $T_{12}$ ,  $A_1$  is stored at  $BF_1$  ( $BF_1$  capacity = 1 unit). In  $T_{13}$ ,  $R_2$  goes at  $P_2$ , while  $R_4$  goes at  $P_3$ . In  $T_{14}$ , the process at  $P_2$  is started utilizing 1 unit from  $BF_1$  ( $BF_1$  capac. = 0), while the process at  $P_3$  is started utilizing 1 unit from  $BF_2$  ( $BF_2$  capac. = 0). In  $T_{15}$ ,  $A_2$  is produced at  $P_2$  after 4 hours, while  $A_3$  is produced at  $P_3$  after 5 hours. In  $T_{16}$ ,  $A_2$  are stored at  $BF_2$  ( $BF_2$  capac. = 1 unit). In  $T_{17}$ ,  $A_3$  are stored at  $BF_3$  ( $BF_3$  capac. = 1 unit), while  $R_4$  goes at  $P_4$ . In  $T_{18}$ , procedure in  $P_4$  is started utilizing  $A_3$  from  $BF_3$ , while  $R_2$  goes at  $P_3$ . In  $T_{19}$ ,  $A_4$  is produced after 7 hours, while  $A_3$  is produced after 5 hours. In  $T_{20}$ ,  $A_3$  are stored at  $BF_3$  ( $BF_3$  capac. = 1 unit). In  $T_{21}$ ,  $A_4$  is stored at  $BF_4$  ( $BF_4$  capac. = 1 unit). In  $T_{22}$ ,  $R_3$  goes at  $P_4$ . In  $T_{23}$ , procedure in  $P_4$  is started utilizing  $A_3$  from  $BF_3$ . In  $T_{24}$ ,  $A_4$  is produced after 7 hours. In  $T_{25}$ ,  $A_4$  is stored at  $BF_4$  ( $BF_4$  capac. = 2 units).

In this case, the cardinality of the environment state space is 1,640,250 states. The time required to construct the environment and the agent models is  $4.35 \times 10^{-5}$  seconds. The runtime to calculate the solution is  $1.004 \times 10^{-3}$  seconds. The time required to fulfill the objective is 37 hours utilizing 6 robots for the whole process with concurrent task execution.

In case there is not a concurrent task execution, then the objective is fulfilled in 32 steps while the time required to fulfill the objective is 46 hours. The robots are grouped in 3 teams of 2. The first team  $R_2$  of 2 robots will be utilized for 13 hours. The second team  $R_3$  of 2 robots will be utilized for 12 hours. The third team  $R_4$  of 2 robots will be utilized for 7 hours. Each team will be utilized for 14 hours more, since processes in  $P_1$  requires 6 robot. So, that is 27 hours in total for the team  $R_2$ , 26 hours in total for the team  $R_3$ , 21 hours in total for the team  $R_4$ .

### B. Case study A-II

For the second case study A, we considered 13 agents; material  $A_0$ , semi-finished products  $A_1$ ,  $A_2$ ,  $A_3$ , final product  $A_4$ , buffer zones  $BF_1$ ,  $BF_2$ ,  $BF_3$ ,  $BF_4$ , 8 robots in total grouped in 4 teams of 2 robots  $R_2$ ,  $R_3$ ,  $R_4$ ,  $R_5$ . The 3 teams together could perform actions in work-cell  $P_1$ , since 6 robots are required. However, each team is allowed to perform actions in work-cells  $P_2$ ,  $P_3$  and  $P_4$ , since 2 robots are required in each work-cell. The capabilities and

constraints of robots team  $R_5$  are modeled as in Fig. 3b and Fig. 4b, respectively. The objective is to produce 2 units of  $A_4$  and locate it at  $BM4$  utilizing the 8 robots in the production line.

In the solution computed by SPECTER, the objective is fulfilled in 22 steps. The 3 teams of 4 could handle the procedure in  $P_1$ , while all teams are able to handle the procedures in  $P_2$ ,  $P_3$  and  $P_4$ .

In this case, the cardinality of the environment state space is 8,201,250 states. The time required to construct the environment and the agent models is  $1.7 \times 10^{-6}$  seconds. The runtime to calculate the solution is  $3.6 \times 10^{-3}$  seconds.

The time required to fulfil the objective is 25 hours utilizing 8 robots grouped in 4 teams of 2 robots for the whole process. The robots of teams  $R_2$ ,  $R_3$  and  $R_4$  will be utilized for 14 hours to perform processes in  $P_1$ . The team  $R_3$  will be utilized for 10 hours more to perform actions in  $P_3$ . The robots of team  $R_5$  will be utilized for 22 hours.

### C. Case study A-III

For the 3rd case study A, we considered 14 agents; material  $A_0$ , semi-finished products  $A_1$ ,  $A_2$ ,  $A_3$ , final product  $A_4$ , buffer zones  $BF_1$ ,  $BF_2$ ,  $BF_3$ ,  $BF_4$ , 10 robots in total grouped in 5 teams of 2 robots,  $R_1$ ,  $R_2$ ,  $R_3$ ,  $R_4$  and  $R_5$ . The objective is to produce 2 units of  $A_4$  and locate it at  $BM4$  utilizing the 10 robots in the production line. The objective is to produce 2 units of  $A_4$  and locate it at  $BM4$  utilizing the 10 robots in the production line. In this case, the cardinality of the environment state space is 41,006,250 states and the runtime exceeded the computational time limit.

### D. Case Study B-I

In the case study B-I, we considered 11 agents; material  $A_0$ , semi-finished products  $A_1$ ,  $A_2$ ,  $A_3$ , final product  $A_4$ , buffer zones  $BF_1$ ,  $BF_2$ ,  $BF_3$ ,  $BF_4$ , 8 robots in total grouped in the team  $R_1$  of 6 robots and team  $R_2$  of 2 robots. The team  $R_1$  could perform action only in work-cell  $P_1$ , whereas  $R_2$  is allowed to perform actions in work-cells  $P_2$ ,  $P_3$  and  $P_4$ . The objective is to produce 2 units of  $A_4$  and locate it at  $BM4$  utilizing the 8 robots in the production line.

In the solution computed by SPECTER, the objective is fulfilled in 25 steps. The team  $R_1$  is handling the procedure in  $P_1$ , while the team  $R_2$  is handling the procedures in  $P_2$ ,  $P_3$  and  $P_4$ . The time required to fulfil the objective is 39 hours. The robots of  $R_1$  will be utilized for 14 hours, while the robots of  $R_2$  will be utilized for 32 hours.

The cardinality of the environment state space is 131,220 states. The time required to construct the environment and the agent models is  $6.27 \times 10^{-3}$  seconds. The runtime to calculate the solution is 72 seconds.

### E. Case study B-II

In the case study B-II, we considered 13 agents; material  $A_0$ , semi-finished products  $A_1$ ,  $A_2$ ,  $A_3$ , final product  $A_4$ , buffer zones  $BF_1$ ,  $BF_2$ ,  $BF_3$ ,  $BF_4$ , 10 robots in total grouped in one team  $R_1$  of 6 robots, 2 teams  $R_2$  and  $R_3$  of 2 robots. The objective is to produce 2 units of  $A_4$  and

Case Study	No. agents	of No. teams of robots	No. of 6 teams of robots	of 2 Space (states)	Time Costs (hours)
A-I	12	0	3	1,640,250	37
A-II	13	0	4	8,201,250	25
A-III	14	0	5	41,006,250	Runtime limit exceeded
B-I	11	1	1	131,220	39
B-II	13	1	2	656,100	25

TABLE II: Case studies parameters.

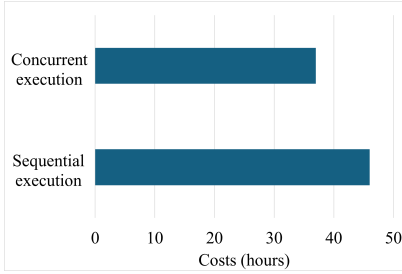


Fig. 9: Costs for the case study A engaging 6 robotic agents.

locate it at  $BM4$  utilizing the 6 robots in the production line. The objective is to produce 2 units of  $A_4$  and locate it at  $BM4$  utilizing the 10 robots in the production line.

In the solution computed by SPECTER, the objective is fulfilled in 22 steps. The team  $R_1$  is handling the procedure in  $P_1$ , while the teams  $R_2$  and  $R_3$  are handling the procedures in  $P_2$ ,  $P_3$  and  $P_4$ . The time required to fulfill the objective is 25 hours. The team  $R_1$  will be utilized for 14 hours, the team  $R_2$  will be utilized for 22 hours and the team  $R_3$  will be utilized for 10 hours.

The cardinality of the environment state space is 656, 100 states. The time required to construct the environment and the agent models is  $2,4 \times 10^{-3}$  seconds. The runtime to calculate the solution is 371 seconds.

## VI. CONCLUSIONS

The outline of the scenarios parameters are summarized in the Table II. The chart of Fig. 10 illustrates the production time for each case study as described in the section V.

As expected, a decrease in the environment state space is observed when the abstraction with the team of 6 robots is utilized. In Fig. 9, the time required to produce 2 units

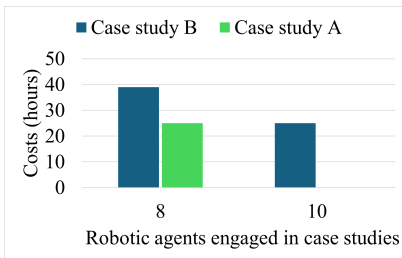


Fig. 10: Costs (hours) for the case studies depending on the number of robotic agents utilized in each case study.

of final product engaging 6 robotic agents requires 46 hours with sequential task execution whereas 37 hours are needed with concurrent task execution.

In Fig. 10, results of case studies A and B are depicted. Two different workflow abstractions are constructed engaging 8 and 10 robotic agents in the production line. A reduction in production time is observed when the robotic agents are grouped in teams of 2 agents while an increase in the state space is registered. Interestingly a decrease in the production time was observed with 8 robots in the production line but no changes were registered when 10 robotics agents engaged. Also, the different abstractions of the workflow do not affect the time required for the production of the final product. This concludes that the optimal (with respect to our case studies) number of robots needed for the production of 2 units of the final product are 8 robots, requiring 25 hours. Further optimizations can be investigated given additional computational resources (e.g. utilizing the complete instead of the heuristic solver of [13]).

## REFERENCES

- [1] C. Galindo, J.-A. Fernandez-Madriral, and J. Gonzalez, "Improving efficiency in mobile robot task planning through world abstraction," *IEEE Transactions on Robotics*, vol. 20, no. 4, pp. 677–690, 2004.
- [2] C. Belta, V. Isler, and G. J. Pappas, "Discrete abstractions for robot motion planning and control in polygonal environments," *IEEE Transactions on Robotics*, vol. 21, no. 5, pp. 864–874, 2005.
- [3] M. Kloetzer and C. Belta, "Temporal logic planning and control of robotic swarms by hierarchical abstractions," *IEEE Transactions on Robotics*, vol. 23, no. 2, pp. 320–330, 2007.
- [4] N. T. Dantam, Z. K. Kingston, S. Chaudhuri, and L. E. Kavraki, "An incremental constraint-based framework for task and motion planning," *The International Journal of Robotics Research*, vol. 37, no. 10, pp. 1134–1151, 2018.
- [5] J. A. DeCastro, V. Raman, and H. Kress-Gazit, "Dynamics-driven adaptive abstraction for reactive high-level mission and motion planning," in *2015 IEEE International Conference on Robotics and Automation (ICRA)*, pp. 369–376, IEEE, 2015.
- [6] J. McMahon and E. Plaku, "Sampling-based tree search with discrete abstractions for motion planning with dynamics and temporal logic," in *2014 IEEE/RSJ International Conference on Intelligent Robots and Systems*, pp. 3726–3733, IEEE, 2014.
- [7] A. Curtis, T. Silver, J. B. Tenenbaum, T. Lozano-Pérez, and L. Kaelbling, "Discovering state and action abstractions for generalized task and motion planning," in *Proceedings of the AAAI conference on artificial intelligence*, vol. 36, pp. 5377–5384, 2022.
- [8] "Gurobi optimization." Available at URL: <https://www.gurobi.com/>, 2023. [Online]. Accessed: 30 March 2024.
- [9] "Nvidia cuOpt." Available at URL: <https://www.nvidia.com/en-us/ai-data-science/products/cuopt/>, 2024. [Online]. Accessed: 30 March 2024.
- [10] M. Aramon, G. Rosenberg, E. Valiante, T. Miyazawa, H. Tamura, and H. G. Katzgraber, "Physics-inspired optimization for quadratic unconstrained problems using a digital annealer," *Frontiers in Physics*, vol. 7, p. 48, 2019.
- [11] S. Tanaka, Y. Matsuda, and N. Togawa, "Theory of ising machines and a common software platform for ising machines," in *2020 25th Asia and South Pacific Design Automation Conference (ASP-DAC)*, pp. 659–666, IEEE, 2020.
- [12] "OpenJij." Available at URL: <https://www.openjij.org/>, 2023. [Online]. Accessed: 30 March 2024.
- [13] A. A. Tziola and S. G. Loizou, "Autonomous task planning for heterogeneous multi-agent systems," in *2023 IEEE International Conference on Robotics and Automation (ICRA)*, pp. 3490–3496, 2023.
- [14] A. A. Tziola and S. G. Loizou, "Manufacturing logistics optimization using the specter task planner: A shoe manufacturing logistics case study," in *2024 European Robotics Forum (ERF)*, 2024.